



Macromolecular Nanotechnology

Polyacrylate/silica nanocomposite materials prepared by sol–gel process

Jian-Zhong Ma, Jing Hu *, Zhi-Jie Zhang

College of Resource and Environment, Shaanxi University of Science and Technology, Xi'an, Shaanxi 710021, People's Republic of China

Received 29 March 2007; received in revised form 25 June 2007; accepted 29 June 2007

Available online 27 July 2007

Abstract

Polyacrylate/silica nanocomposite was prepared by sol–gel process via in situ emulsion polymerization. The influence of the synthetic conditions, such as the ratio of different monomers and the contents of tetraethoxysilane (TEOS), γ -methacryloxypropyltrimethoxysilane (Z-6030), diethanolamine (DAM) and ammonium persulfate (APS) on the physical mechanical properties of polyacrylate/silica nanocomposite was investigated in details. Dynamics Laser Scattering (DLS) indicated that the average diameter of the polyacrylate/silica latex particles (177 nm) was bigger than that of the pure polyacrylate latex particles (105.3 nm), but the ζ potential of polyacrylate/silica was decreased respectively in contrast to that of the polyacrylate. Differential Scanning Calorimeters (DSC) analysis confirmed that the glass transition temperature of polyacrylate/nano-SiO₂ ($T_g = -24$ °C) was higher than that of polyacrylate ($T_g = -36$ °C). UV analysis showed that the UV absorbency of polyacrylate/silica was improved evidently in contrast to that of polyacrylate.

© 2007 Elsevier Ltd. All rights reserved.

Keywords: Polyacrylate; Silica; Sol–gel process; Nanocomposite

1. Introduction

In recent years, organic–inorganic hybrid materials are of growing interest because they display enhanced or even novel properties in both mechanical and calorifics, which is attributed to the nanoeffect and strong chemical coalescents between the nanoparticles and polymer [1–9]. Especially silica-based organic–inorganic hybrid materials can be potentially used in many fields such as plastics, rubbers, coatings, etc. [10–13]. Zhang [14] prepared

poly (methacrylic methacrylate) (PMMA)/silica hybrid materials via sol–gel process, which possessed the high transparency and heat-stability. Bokobza et al. [15] reported that silica sol modified by silane coupling agents was mixed with the acrylate monomers to obtain the silica-based hybrid films by ultraviolet radiation. Chen et al. [16] prepared polyester or polyester-based polyurethane/silica hybrid material obtained by sol–gel process.

Up to now, polyacrylate/silica nanocomposite has been widely used in the building fields. The uniform dispersal of nano-SiO₂ in the polymer can improve the strength, the abrasion-resistance, the aging-resistance and the climate-resistance of the polymer materials. However, there are few researches about

* Corresponding author. Tel.: +86 2986168010; fax: +86 2986168012.

E-mail address: hujing616@gmail.com (J. Hu).

polymer/silica nanocomposite in the leather finishing agent. In our previous papers [17,18], two types of nano-silica sols obtained under acidic and alkali condition via sol-gel process were mixed with the acrylic resin to prepare acrylic resin/nano-SiO₂ composite. Here we prepare polyacrylate/silica nanocomposite via sol-gel process by in situ emulsion polymerization. The influence of the synthetic conditions such as the ratio of the monomers, the contents of TEOS, Z-6030, DAM and APS on the properties of polyacrylate/silica nanocomposite is investigated.

2. Experimental

2.1. Materials

TEOS (tetraethoxysilane), ammonium hydroxide (25 wt%), MMA, butyl acrylate (BA), diethanolamine (DAM), sodium dodecyl sulfate (SDS), nonyl phenyl polyoxyethylene ether-10 (OP-10) and ammonium persulfate (APS) were all purchased from Tianjin No. 3 Chemical Reagent Factory and used without further purification. γ -Methacryloxypropyltrimethoxysilane (Z-6030) was analytically pure and provided by American Dorwing Ltd.; Dionized water was applied for the polymerization processes.

2.2. Preparation of polyacrylate/silica nanocomposite

The procedure for preparing polyacrylate/silica nanocomposite is schematically shown in Fig. 1. In a typical experiment, SDS, OP-10 (the molar ratio of SDS and OP-10 is 1:2) and dionized water

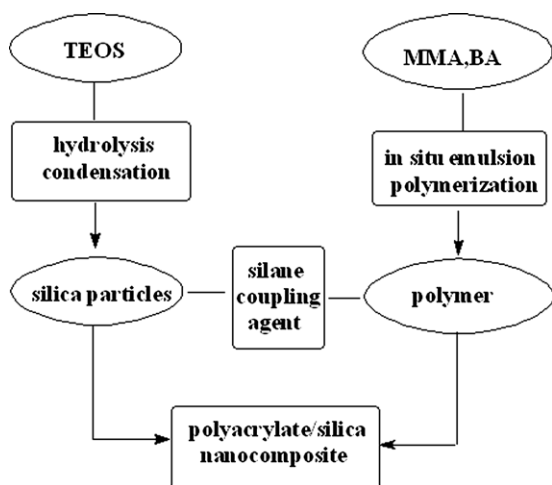


Fig. 1. The procedure for preparing polyacrylate/silica nanocomposite.

(80 g) were charged into a 500-ml 3-necked round-bottom flask equipped with a reflux condenser, a thermometer and a magnetic stirring bar and were heated to 40 °C under stirring for 30 min; After TEOS (variable), Z-6030 (variable) and DAM (variable) introduced into the flask for 15 min, the mixture 13 g of MMA and BA, 10 g aqueous solution of APS (variable) was charged to the reactor for 30 min at 80 °C. Then, the polymerization was started with 20 g aqueous solution of APS (variable) and the monomers added dropwise and finished within 1 h. The reaction was kept at 85 °C for 2 h. (The contents of SDS and OP-10, TEOS, Z-6030, DAM and APS were based on the monomers.)

2.3. Determination of physical mechanical property of composite films

2.3.1. Determination of solid content

A weighing bottle was placed into the oven (DHG-101A-1B Galvanothermy Constant Temperature Air-dry Oven, Shanghai Shendang Electricity Factory) at 100 ± 2 °C for 6 h. Next it was put into a desiccator to cool for 30 min and then weighed. It was again allowed to dry in the oven for 1 h and cool until the constant weight was obtained. Weighing bottle filled with 3.000 g polyacrylate/silica nanocomposite (exactly to 0.0002 g, the error allowance were not more than 0.3%) were placed into oven at 100 ± 2 °C for 6 h and the same procedure as outlined above was followed [19].

$$\text{Solid content} = [m_1 - m_0] / m \times 100\%$$

m_1 is the specimen mass after constant weightness (including weighing bottle mass); m_0 the weighing bottle mass after constant weight and m is the specimen mass.

2.3.2. Preparation of composite films

Composite emulsion was weighed (the same mass based on solid content), poured into an orbicular glass service (120 mm diameter), and laid on the horizontal surface until emulsion became films.

2.3.3. Sampling

The films were sampled with the standard mould as shown in Ref. [20] (the models of tensile strength were dumbbell forms with 80 mm span and 5 mm middle breadth; those of slit strength were rectangle of hexagon barren in middle with 50 mm span and 25 mm breadth). Then samples were kept at 20 ± 2 °C and relative humidity (60–70%) for 4 h.

2.3.4. Determination of tensile strength

The thickness of the films in the midline was measured via YQ981 Leather Thickness Measure Instrument made by Middle Mountain Sword Tool Factory. The measuring points were chosen more than 3 and then the average was obtained. Samples were fixed between the clamps of GFU55 Functional Materials Examination Machine made by Taiwan High Iron Science and Technology Stock Company (extending speed 500 mm/min, backhaul speeding 100 mm/min) and determined. The burthen number at break was recorded.

$$X = F/S$$

X is the tensile strength of specimen (N/mm^2); F the burthen number at break (N) and S is the transect acreage at break (mm^2).

2.3.5. Determination of elongation at break

Elongation at break was determined during the measure of tensile strength. When the specimen was extended, the distance between the two standard lines was recorded.

$$X = [L_1 - L]/L \times 100\%$$

X is the elongation at break (%); L_1 the distance between midline of specimen at break (mm) and L is the distance between midline of former samples (mm).

2.3.6. Determination of slit strength

The thicknesses of the films at points A and B were determined. Then the specimens were installed between the clamps of Functional Materials Examination Machine. The bend clasp was towards outside. When one end of specimen was slit, the highest burthen number was recorded.

$$p = F \times 10/D$$

p is the slit strength (N/mm); F the highest number (N); D is the thickness of specimen (A or B) (mm).

The above samples were parallel experiments including two groups; the result was obtained from the average numerical value. The error allowance was not more than 10%.

2.4. Bromine value of emulsions

0.4–0.6 g specimens (exactly to 0.0002 g) were added into 250 ml conical flask charged with 60 ml

aqueous solution of sodium dodecyl sulphonate (5 wt%). 25 ml aqueous solution of $\text{KBr}-\text{KBrO}_3$ (0.01 mol/l) was also put into the flask. After 10 ml aqueous solution of HCl (1:1) poured into along the flask wall, the flask was sealed with 10 ml aqueous solution of KI (10 wt%) and placed for 30 min in the dark. $\text{Na}_2\text{S}_2\text{O}_3$ standard solution (0.05 mol/l) was in titration with 2 ml starch as the indicator. The content of $\text{Na}_2\text{S}_2\text{O}_3$ was recorded at the end of the titration. Blank experiment was done as the above without the specimen [19].

$$X = (V_0 - V) \times c \times 79.9 \times 100 / (1000 \times W)$$

X is the bromine value (%); V_0 the volume of $\text{Na}_2\text{S}_2\text{O}_3$ standard solution used in blank experiment (ml); V the volume of $\text{Na}_2\text{S}_2\text{O}_3$ standard solution used in specimens (ml); c the concentration of $\text{Na}_2\text{S}_2\text{O}_3$ standard solution (mol/l); W the sample mass (g); 79.9 is the molar mass of bromine.

* is the error of twice parallel experiment results is not more than 0.1%.

2.5. Characterization

2.5.1. FTIR analysis

Fourier transform infrared spectrometer (FTIR) analysis of the polyacrylate and polyacrylate/silica films after the solvent (anhydrous ethanol) purification was performed by VETOR-2 FTIR (Bruker Company in German).

2.5.2. DLS analysis

The average diameter and the ζ potential of the polyacrylate and polyacrylate/silica latex particles were obtained by a Zetasizer Nano ZS (Malvern Instruments Ltd., UK).

2.5.3. UV analysis

The absorbance of the polyacrylate and polyacrylate/silica films in the range of 190–900 nm wavelength light was determined with a 61 CRT Spectrophotometer (Shanghai Instrument Factory, China).

2.5.4. Thermal analysis (DSC)

Differential Scanning Calorimeters analysis was carried out on SHIMADZU DSC-50 (Netzsch Company in German). The samples were quickly cooled to -50°C and equilibrated at that temperature for 3 min, then heated to 300°C at the scan rate of $5^\circ\text{C}/\text{min}$ under nitrogen atmosphere.

3. Results and discussion

3.1. The Mechanism of polyacrylate/silica nanocomposite

The whole polymerization procedure includes both the free radical polymerization reaction of acrylate monomers and the hydrolysis condensation reaction of TEOS, which belongs to the chain polymerization and step polymerization. The acrylate monomers, TEOS and Z-6030 disperse sufficiently and are embedded into the emulsions micelles; the nanocomposite materials of good miscibility are obtained by the synthesis of silica particles and the polymerization of the monomers. When nano-silica particles disperse in the resin, $-OH$ groups on those should function with the chain of polyacrylate chemically; organic components and inorganic ones bond with each other by the bridge of Z-6030, which contains an “ $-C=CH_2$ ” group, Fig. 2 shows the ideal mechanism of polyacrylate/silica nanocomposite.

3.2. Effect of the MMA/BA ratios

Table 1 demonstrates that the properties of polyacrylate/silica nanocomposite obtained with different MMA/BA molar ratios. The solid contents of polyacrylate/silica are almost kept invariable; obviously, the ratios of MMA to BA have a drastic impact on the physical mechanical properties of nanocomposite. The incorporation of the hard monomer (MMA) results in the rigidity and the good adhesion of the polyacrylate/silica nanocomposite. However, the flexibility of the polyacrylate/silica nanocomposite is improved while the strength of that decreased with the incorporation of the soft monomer (BA).

3.3. Effect of APS contents

Table 2 shows that the influence of different APS contents on the properties of the nanocomposite emulsion. The polymer of the high molecular weight and regular structure is obtained with small APS

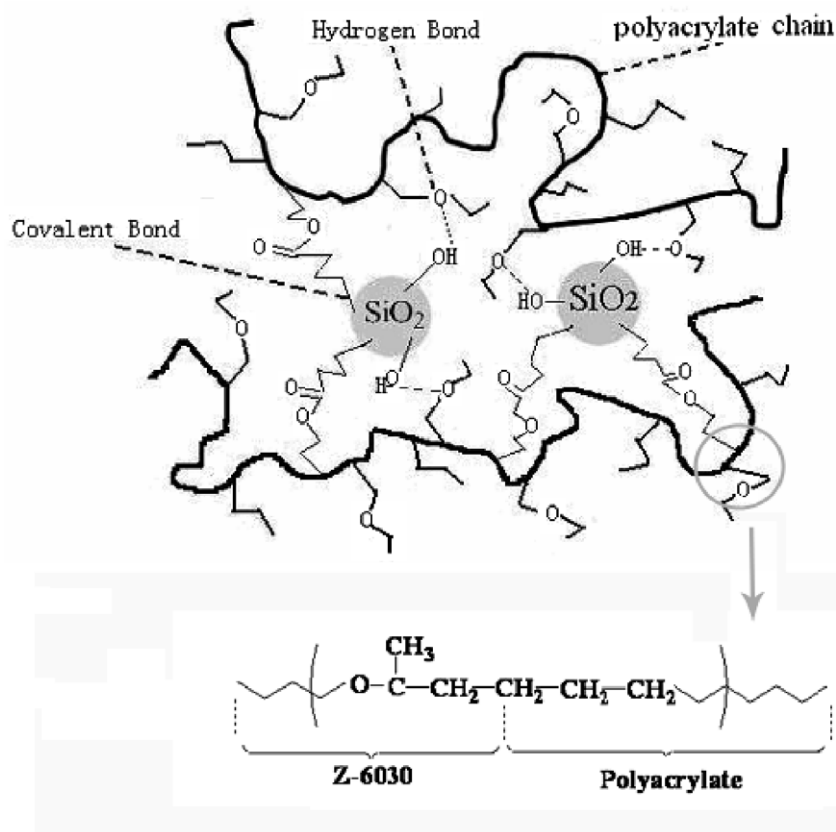


Fig. 2. The ideal mechanism of polyacrylate/silica nanocomposite.

Table 1
 Proyacrylate/silica nanocomposite properties at different MMA/BA molar ratios

$n(\text{MMA}):n(\text{BA})$	Tensile strength (N/mm ²)	Slit strength (N/mm)	Elongation at break (%)	Bomine value (24 h)	Solid content (wt%)
1:1	1.853	3.133	44.92	3.40	21.57
1:2	2.796	1.517	106.86	1.34	21.95
1:3	0.997	0.397	78.56	1.85	21.33
1:4	0.910	0.254	42.46	1.44	22.18
1:5	0.909	0.238	54.21	3.45	23.17

Table 2
 Proyacrylate/silica nanocomposite properties at different contents of APS

APS (mt%)	Tensile strength (N/mm ²)	Slit strength (N/mm)	Elongation at break (%)	Bomine value (24 h)	Solid content (wt%)
0.5	6.65	7.014	377.75	2.90	22.41
1.5	–	–	–	2.86	22.25
2.5	1.92	6.65	300.11	1.33	21.17
4.0	2.055	2.823	178.22	4.58	21.57

“–” shows the instability of polyacrylate/silica.

content. In reverse, that of the low molecular weight and complex structure is obtained. In the meanwhile, the hydrolysis and condensation of TEOS can depend on the large use of APS, but not demand the higher temperature and the longer time. Here APS is used to be polymerized under 80 °C. When the large amount of APS (4 mt%) is used, the properties of nanocomposite decrease, which is because the dispersal of inorganic materials and the polymerization of organic macromolecule are not carried out at the same time.

3.4. Effect of emulsifier contents

Table 3 demonstrates that the properties of nanocomposites decrease with the contents of the emulsifiers increasing. The emulsifiers not only determine the even dispersal between the acrylate monomers and nano inorganic precursor, but also offer the reaction room to the polymerization of the monomers and the hydrolysis and condensation of TEOS.

Nano-silica particles should be obtained when TEOS is distributed into the micelles uniformly. As seen from Table 3, polyacrylate/silica cannot film using 6 mt% emulsifiers, which is belongs to the reduction of the acrylate monomers polymerization in the micelles.

3.5. Effect of TEOS contents

There are two parts of TEOS in the reaction system. One part of TEOS and the acrylate monomers is embedded into the emulsifier micelles; the other is dissociated outside of the micelles. The hydrolysis and the condensation of TEOS in the micelles are carried out with the polymerization of the monomers to realize in situ polymerization of organic and inorganic materials, but those of TEOS outside the micelles cannot composite with the organic materials equably to produce the gel or the deposition. Table 4 shows the properties of the nanocomposite decrease as the increase of TEOS contents.

Table 3
 Proyacrylate/silica nanocomposite properties at different contents of emulsifiers

Emulsifier (mt%)	Tensile strength (N/mm ²)	Slit strength (N/mm)	Elongation at break (%)	Bomine value (24 h)	Solid content (wt%)
3	1.918	6.79	596.56	1.46	22.19
4	1.864	7.02	178.58	3.40	21.57
5	1.89	6.68	302.19	2.13	20.87
6	–	–	–	1.15	23.06

“–” shows the instability of polyacrylate/silica.

Table 4
Proyacrylate/silica nanocomposite properties at different contents of TEOS

TEOS (mt%)	Tensile strength (N/mm ²)	Slit strength (N/mm)	Elongation at break (%)	Bomine value (24 h)	Solid content (wt%)
1	4.519	3.540	97.21	2.52	20.73
3	3.077	3.204	97.46	2.65	20.54
5	2.624	2.811	98.41	2.46	22.08
7	1.853	2.133	44.92	3.40	21.57

“–” shows the instability of polyacrylate/silica.

The reason for this is that the contents of the emulsifier limit the existence of TEOS in the micelles. The large part of TEOS outside has become the gel.

3.6. Effect of Z-6030 contents

The influence of the different Z-6030 contents on the properties of the nanocomposite is shown in Table 5. The modified silica using silane coupling agent promotes the miscibility between the hydrophilic inorganic silica phase and the hydrophobic organic phases. The function mechanism of the silane coupling agent with silica is shown in Fig. 3.

When a great number of Z-6030 are used in the reaction, the overabundant bridge bonds between the inorganic and the organic materials formed

result in the increase of the brittleness of the polymer and the decrease of the physical mechanical properties. There is a lot of the ropy matter in the emulsion during the reaction with 9 mt% of the silane coupling agents introduced.

3.7. Effect of DAM contents

Table 6 represents the effect of DAM contents on the properties of the nanocomposite. The best property of the nanocomposite is obtained with 2 mt% of DAM used in the reaction. The main function of DAM is the inhibitor of the hydrolysis and the condensation of inorganic materials precursor and pH regulator of the organic monomers polymerization. The introduction of DAM can improve the physical

Table 5
Proyacrylate/silica nanocomposite properties at different contents of silane coupling agent

Silane coupling agent (mt%)	Tensile strength (N/mm ²)	Slit strength (N/mm)	Elongation at break (%)	Bomine value (24 h)	Solid content (wt%)
1	–	–	–	1.44	21.21
3	1.853	3.133	44.92	3.40	21.57
5	4.910	5.078	72.88	3.75	19.60
7	4.878	2.427	59.28	1.02	24.13

“–” shows the instability of polyacrylate/silica.

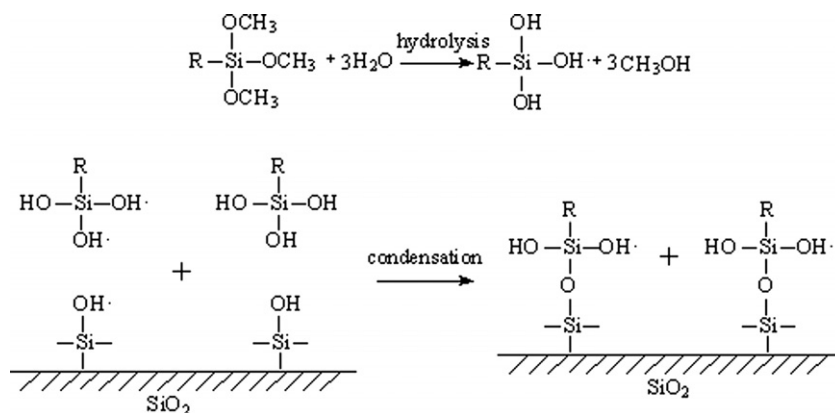


Fig. 3. The function mechanism of silane coupling agent with silica.

Table 6
 Proyacrylate/silica nanocomposite properties at different contents of DAM

DAM (mt%)	Tensile strength (N/mm ²)	Slit strength (N/mm)	Elongation at break (wt%)	Bomine value (24 h)	Solid content (wt%)
0	1.853	1.113	44.92	3.40	21.57
1	1.994	3.314	163.825	2.65	22.45
2	4.001	2.000	109.315	1.46	22.08
3	–	–	–	2.70	21.57
4	–	–	–	3.52	20.73

“–” shows the instability of polyacrylate/silica.

mechanical properties of the nanocomposite evidently. It does not show that small amount of DAM inhibit the hydrolysis and the condensation of inorganic materials, while the large amounts cause the system instable during the polymerization.

3.8. FTIR analysis

Fig. 4 displays the differences between the structures of polyacrylate and polyacrylate/silica. In FTIR spectrum of polyacrylate/silica, the absorption peaks 3441.83 cm⁻¹ and 3210.20 cm⁻¹ are affected by extending vibration of Si–OH. The absorption peaks of 1065.20 cm⁻¹ and 1024.12 cm⁻¹ belong to extending vibration of Si–O–Si.

3.9. DLS analysis

Figs. 5a, 5b and Table 7 demonstrate the great difference between the polyacrylate and the polyacrylate/silica latex particles. The average diameter of the polyacrylate/silica latex particles increase and the polydispersity index of that decrease in contrast to those of the polyacrylate, which is because the former latexes particles include the silica and poly-

acrylate, in addition, there may be the aggregation of nano-silica. The ζ potentials of the polyacrylate and the polyacrylate/silica were determined at pH 7.0. The silica influences the ζ potential of the polyacrylate composite particles strongly. The reason for this is that silica was hence cationic, which results in the positive ζ potential.

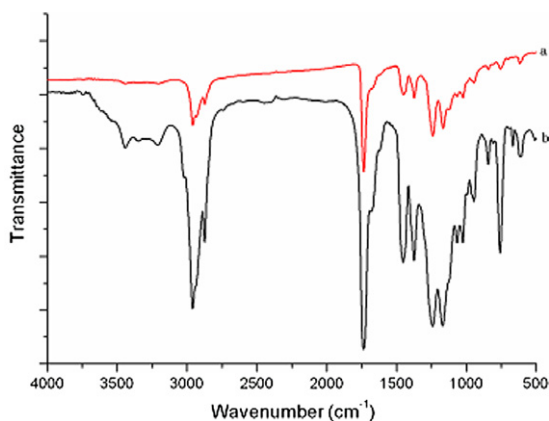


Fig. 4. FTIR analysis (a: polyacrylate, b: polyacrylate/silica).

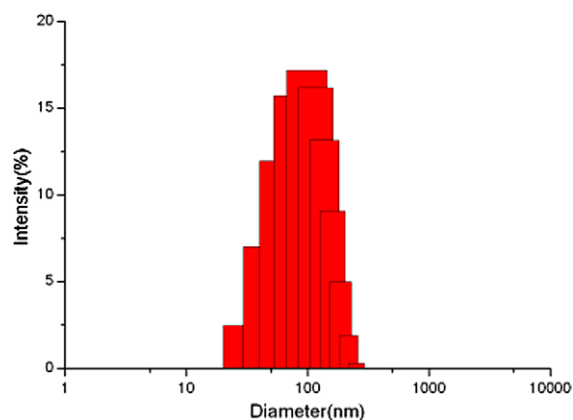


Fig. 5a. The polydispersion of the polyacrylate latex particles.

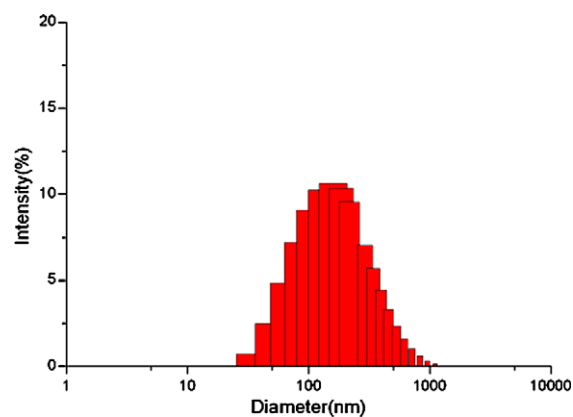


Fig. 5b. The polydispersion of the polyacrylate/silica latex particles.

Table 7

DLS analysis result of polyacrylate and the polyacrylate/silica latex particles

Sample	D (nm)	PI	ζ potential (mv)
a	105.3	0.094	-64.57
b	177	0.198	-20.71

PI: polydispersion index.

3.10. UV-analysis

Fig. 6 illustrates the influence of silica on the UV absorbency of the polyacrylate evidently. The UV absorbency of the polyacrylate/silica via sol-gel process by in situ emulsion polymerization increases in comparison with that of the polyacrylate. That belongs to the existence of nano-silica.

3.11. DSC analysis

Fig. 7 shows that the glass transition temperature (T_g) of the polyacrylate/nano-silica ($T_g = -24^\circ\text{C}$) is higher than that of the polyacrylate ($T_g = -36^\circ\text{C}$). The reason for this is that the incorporation of nano-silica interacts with polymer molecules to restrain the vertical molecule movement of the polyacrylate. T_m of polyacrylate film is about 200°C . When nano- SiO_2 is added into the polyacrylate, T_m of polyacrylate/silica film has disappeared, which shows that the transparency of the polyacrylate/silica films can be improved in contrast to polyacrylate films. The existence of only one T_g in the polyacrylate/silica demonstrates the organic materials and inorganic ones combined chemically.

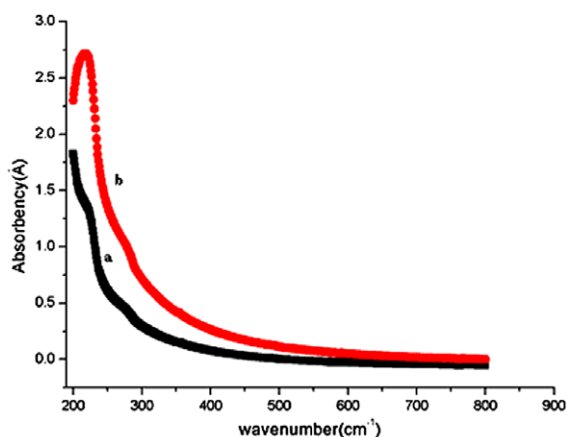


Fig. 6. UV analysis (a: polyacrylate, b: polyacrylate/silica).

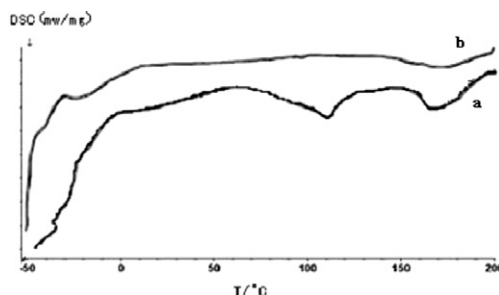


Fig. 7. DSC picture (a: polyacrylate, b: polyacrylate/silica).

4. Conclusions

The physical mechanical properties of the polyacrylate/silica nanocomposite prepared via sol-gel process by in situ emulsion polymerization are strongly dependent upon the ratios of different monomers and the contents of TEOS, Z-6030, DAM, and APS. Dynamics Laser Scattering (DLS) indicated that the average diameter of the polyacrylate/silica latex particles (177 nm) was bigger than that of the pure polyacrylate latex particles (105.3 nm), but the ζ potential of polyacrylate/silica was decreased in contrast to that of the polyacrylate. Differential Scanning Calorimeters (DSC) analysis confirmed the glass transition temperature of the polyacrylate/silica ($T_g = -24^\circ\text{C}$) was higher than that of the polyacrylate ($T_g = -36^\circ\text{C}$). UV analysis showed that the UV absorbency of the polyacrylate/silica was improved evidently in contrast to that of the polyacrylate.

Acknowledgements

This investigation was supported by Ministry of Education New Century Excellent Talents Foundation of China (Item No.: NCET-04-0973), National Natural Science Foundation (Item No.: 20674047) and the Team Work Project of Science Innovation of Shaanxi University of Science and Technology (Item No.: SUST-A03).

References

- [1] Bauer F, Sauerland V, Glasel HJ, et al. *Macromol Mater Eng* 2002;287:546–52.
- [2] Zhang LD, Mou JM. *Nanomaterials and nanostructure*. Beijing: Science Press; 2001. p. 108–109.
- [3] Rong MZ, Zhang MQ, Pan SL, et al. *J Appl Polym Sci* 2004;92:1771–81.
- [4] Yu YJ, Yang CQ, Gao Y, et al. *J Polym Sci Part A: Polym Chem* 2005;43:6105.

- [5] Erdem B, Sudol ED, Dimonie VL, et al. *J Polym Sci Part A: Polym Chem* 2000;38:4419–30.
- [6] Erdem B, Sudol ED, Dimonie VL, et al. *J Polym Sci Part A: Polym Chem* 2000;38:4431–40.
- [7] Yu J, Guo ZX, Gao YF. *Macromol Rapid Commun* 2001;22:1261–4.
- [8] Duguet E, Abboud M, Morvan F, et al. *Macromol Symp* 2000;151:365–70.
- [9] Zeng Z, Yu J, Guo ZX. *J Polym Sci Part A: Polym Chem* 2005;43:2826–35.
- [10] Lee MS, Jo NJ. *J Sol–Gel Sci Tech* 2002;24:175–80.
- [11] Zhou J, Zhang SW, Qiao XG, et al. *J Polym Sci Part A: Polym Chem* 2006;44:3202–9.
- [12] Yu YY, Chen CY, Chen WC. *Polymer* 2003;44:593–601.
- [13] Carrot G, Diamanti S, Manuszak M, et al. *J Polym Sci Part A: Polym Chem* 2001;39:4294–301.
- [14] Zhang QW, Zhang YH, Chen SM, et al. *Appl Chem* 2002;19(9):874–7.
- [15] Bokobza L, Gamaud G, Mark JE. *Chem Mater* 2002;14:162–7.
- [16] Chen YC, Zhou SX, Yang HH, et al. *J Sol–Gel Sci Tech* 2006;37:39–47.
- [17] Ma JZ, Zhang ZJ, Liu LY, et al. *JSLTC* 2006;90(4):188–92.
- [18] Ma JZ, Hu J, Zhang ZJ. *J Composite Mater* 2006;40(24):2189–201.
- [19] Pan JS, Yang ZS. *Leather analysis and measurement*. Beijing: China Light Industry Press; 1979.
- [20] National Quality Standards Department of Light Industry Bureau. *China light industry standards of leather[M]*. Beijing: China Standards Press; 1999.